Histochemistry and Cell Biology (2021) 155:391–404
https://doi.org/10.1007/s00418-020-01943-0

ORIGINAL PAPER

Cluster of differentiation (CD) 9-positive mouse pituitary cells are adult stem/progenitor cells

Kotaro Horiguchi[1] · Saishu Yoshida[2] · Takehiro Tsukada[3] · Ken Fujiwara[4] · Takashi Nakakura[5] · Rumi Hasegawa[1] · Shu Takigami[1] · Shunji Ohsako[1]

Accepted: 9 November 2020 / Published online: 22 November 2020

Abstract

SOX2-positive cells are stem/progenitor cells that supply hormone-producing cells; they are found in the anterior lobe of the rodent pituitary gland. However, they are likely composed of several subpopulations. In rats, a SOX2-positive cell populations can be distinguished by the presence of S100β. We identified the novel markers cluster of differentiation (CD) CD9 and CD81, members of the tetraspanin superfamily, for the identification of S100β/SOX2-positive cells. Recently, CD9/CD81 double-knockout mice were generated. Although they grew normally until 3 weeks after birth, they exhibited atrophy of the pituitary gland. These findings suggested that CD9/CD81/S100β/SOX2-positive cells in the mouse pituitary are adult stem/progenitor cells. To substantiate this hypothesis, we examined CD9 and CD81 expression in the adult and developing anterior lobe. Immunohistochemistry showed that CD9/CD81-positive cells began appearing from postnatal day 0 and settled in the stem cell niches (marginal cell layer and parenchyma) of the adult anterior lobe while expressing S100β. We next isolated CD9 -positive cells from the adult anterior lobe, using the anti-CD9 antibody for cell characterisation. The cells in culture formed free-floating three-dimensional clusters (pituispheres); moreover, induction into all types of hormone-producing cells was successful. Furthermore, reduction of CD9 and CD81 mRNAs by siRNAs inhibited cell proliferation. These findings indicate that CD9/CD81/S100β/SOX2-positive cells may play a role as adult stem/progenitor cells in SOX2-positive subpopulations, thus supplying hormone-producing cells in the postnatal anterior lobe. Furthermore, CD9 and CD81 are implicated in cell proliferation. The current findings provide novel insights into adult pituitary stem/progenitor cells.

Keywords Anterior pituitary gland · CD9 · SOX2 · Stem cells · S100β-protein

Electronic supplementary material The online version of this article (https://doi.org/10.1007/s00418-020-01943-0) contains supplementary material, which is available to authorized users.

✉ Kotaro Horiguchi
kota@ks.kyorin-u.ac.jp

[1] Laboratory of Anatomy and Cell Biology, Department of Health Sciences, Kyorin University, 5-4-1 Shimorenjaku, Mitaka, Tokyo 181-8612, Japan

[2] Department of Biochemistry, The Jikei University School of Medicine, 3-25-8 Nishi-shinbashi, Minato-ku, Tokyo 105-8461, Japan

[3] Department of Biomolecular Science, Faculty of Science, Toho University, 2-2-1 Miyama, Funabashi, Chiba 274-8510, Japan

[4] Department of Biological Science, Kanagawa University, 2946 Tsuchiya, Hiratsuka, Kanagawa 259-1293, Japan

[5] Department of Anatomy, Graduate School of Medicine, Teikyo University, 2-11-1 Kaga, Itabashi, Tokyo 173-8605, Japan

Abbreviations

ACTH	Adrenocorticotropic hormone
AMCA	Dipeptide-β-Ala-Lys-*N*ε-7-amino-4-methylcoumarin-3-acetic acid
BIO	6-Bromoindirubin-3′-oxime
CD	Cluster of differentiation
CD9/CD81/S100β/SOX2-positive	CD9-, CD81-, S100β-, and SOX2-quadruple positive
DAPI	4,6-Diamidino-2-phenylindole
DKO	Double-knockout
ECM	Extracellular matrix
E10.5	Embryonic day 10.5
FBS	Foetal bovine serum
GH	Growth hormone
HE	Haematoxylin–eosin

KSR	KnockOut serum replacement
LH	Luteinising hormone
MCL	Marginal cell layer
POMC	Proopiomelanocortin
PB	Phosphate buffer
PBS	Phosphate buffered saline
PRL	Prolactin
P0	Postnatal day 0
siRNA	Small interfering RNA
SOX2	Sex-determining region Y-box 2
S100β	S100β protein
TSH	Thyroid-stimulating hormone
WT	Wild type

Introduction

The pituitary gland is an endocrine organ that produces many hormones affecting growth, sexual development, metabolism, and reproduction. The rodent pituitary gland is composed of the anterior, intermediate, and posterior lobes. The anterior lobe contains hormone-producing cells together with non-hormonal cells, such as S100β protein (S100β)-positive cells and fenestrated sinusoids (i.e., endothelial cells and pericytes). S100β-positive cells in the anterior lobe are usually referred to as folliculo-stellate cells (Vila-Porcile 1972). Folliculo-stellate cells comprise heterogeneous populations playing multiple biological roles: e.g. stem cells, phagocytes, or cells regulating hormone release in the anterior lobe (Allaerts and Vankelecom 2005).

It is well known that the supply of hormone-producing cells from sex-determining region Y-box 2 (SOX2)-positive stem/progenitor cells is important for sustaining the function of the pituitary gland. Fauquier et al. (2008) demonstrated that *Sox2*-expressing cells isolated from the mouse anterior lobe form characteristic free-floating three-dimensional clusters (pituispheres) and have the capacity to differentiate into all types of endocrine cells (Andoniadou et al. 2013; Fauquier et al. 2008). Our previous studies in rats have shown that SOX2-positive stem/progenitor cells comprise multiple subpopulations defined by the existence of S100β and other factors, such as PROP1, PRX1, and PRX2 (Higuchi et al. 2014; Susa et al. 2012; Yoshida et al. 2011). Recently, we successfully isolated a subpopulation of SOX2-positive cells (cluster of differentiation (CD) 9/CD81/SOX2/S100β-positive cells) from the rat anterior lobe using a monoclonal antibody against CD9. CD9 is a member of the tetraspanin superfamily and forms a complex with CD81. It was also found that these cells could differentiate into endothelial cells (Horiguchi et al. 2018, 2020a). CD9 and CD81 double-knockout (CD9/CD81 DKO) mice generated by Jin et al. (2018) exhibited atrophy of the adult pituitary gland, although the DKO mice developed normally until 3 weeks after birth. Both male and female CD9/CD81 DKO mice displayed progressively decreasing body weight and bone mineral density. The muscle and visceral adipose tissues also had significantly reduced volumes. Furthermore, some phenotypes of CD9 KO and CD81 KO mice were similar to those of CD9/CD81 DKO mice, such as infertility (Jin et al. 2018). These results suggest that both CD9 and CD81 play an important role in the differentiation of S100β/SOX2-positive stem/progenitor cells into hormone-producing cells in the mouse anterior lobe. Thus, in the present study, we tested whether CD9/CD81/SOX2/S100β-positive cells exist in the adult and developing mouse pituitary glands. In addition, using an anti-CD9 antibody, we attempted to isolate CD9-positive cells from the mouse anterior lobe to examine their capacity for pituisphere formation and differentiation into hormone-producing cells.

Materials and methods

Animals

Male Institute of Cancer Research (ICR) mice were purchased from Japan SLC, Inc. (Shizuoka, Japan). 8- to 10-week-old male mice were given food and water ad libitum and housed under a 12 h light/12 h dark cycle. After the mice were mated, the day of vaginal spermatozoa introduction was designated embryo day 0.5 (E0.5), and the day of parturition postnatal day 0 (P0). The present study was approved by the Committee on Animal Experiments of Kyorin University, based on the NIH Guidelines for the Care and Use of Laboratory Animals.

Tissue preparation

Cryosection: Mice were deeply anesthetised with a combination of three anaesthetics (0.15 mg/kg medetomidine, Zenyaku Kogyo, Tokyo, Japan; 2.0 mg/kg midazolam, SANDOZ, Tokyo, Japan; and 2.5 mg/kg butorphanol, Meiji Seika Pharma, Tokyo, Japan), and the pituitary glands were dissected. They were immediately immersed in a fixative consisting of 4% formaldehyde in 0.05 M phosphate buffer (PB; pH 7.4) for 20–24 h at 4 °C. The tissues were incubated in PB (pH 7.2) containing 30% sucrose at 4 °C for more than 2 days. They were then embedded in Tissue Tek O.C.T. compound (Sakura Finetek Japan, Tokyo, Japan) and frozen rapidly. Frozen sagittal (embryonic pituitaries) and frontal sections (postnatal pituitaries) at a thickness of 8 µm were obtained using a cryostat (CM1860, Leica Microsystems, Wetzlar, Germany; Tissue-tek Polar DM, Sakura Finetek

Japan) and mounted on glass slides (Matsunami, Osaka, Japan).

Immunohistochemistry and immunocytochemistry

Immunohistochemistry was performed as described previously (Horiguchi et al. 2018). Primary and secondary antibodies are listed in Table 1. The absence of an observable nonspecific reaction was confirmed using normal mouse, rabbit, or goat serum (Vector Laboratories, Burlingame, CA, USA). Sections were scanned using an epifluorescence microscope (BX61, Olympus, Tokyo, Japan) with the cellSens Dimension system (Olympus). For double immunofluorescence, sections or smear preparations were incubated in phosphate-buffered saline (PBS; pH 7.2) containing 2% normal goat or donkey serum (Vector Laboratories) for 20 min at 30 °C. Nuclei were counterstained by mounting with VECTASHIELD Mounting Medium containing DAPI (Vector Laboratories). After immunohistochemistry, 6 random fields (157.5 × 210 mm rectangle) were captured per section using a 40-fold objective lens. The number of cells positive for hormones and the total number of cells (DAPI) per area were counted with the cellSens Dimension system. Cell counts were performed three times for each experimental group. The absence of an observable nonspecific immunoreaction against CD9 was confirmed using a preabsorption control. Briefly, the anti-CD9 antibody was preincubated with a CD9 peptide (ORB217044; Biobyt, Cambridge, UK) at a molar ratio for 2 days at 4 °C and then centrifuged; the resultant supernatant was used as the preabsorbed antibody.

For immunocytochemistry, cultured cells were fixed with 4% paraformaldehyde in 0.025 M PB for 20 min at room temperature, and then permeabilized with 0.5% Triton X-100 (Sigma-Aldrich, St. Louis, MO, USA) for 2 min at room temperature. Cells were incubated with PBS containing 2% normal goat or donkey serum for 20 min at 30 °C, followed by incubation with primary and secondary antibodies (Table 1).

Isolation of CD9-positive cells

The anterior lobes of adult male mice were dissected, and the cells were dispersed as described previously (Horiguchi et al. 2018, 2020a). Dispersed cells were separated using the Universal pluriBeads kit (pluriSelect) with anti-rat CD9 monoclonal antibody (Santa Cruz Biotechnology, Santa Cruz, CA, USA), as described in our previous papers (Horiguchi et al. 2018, 2020b). CD9-positive and CD9-negative cells were processed for smear preparation, quantitative polymerase chain reaction (qPCR), cultivation, and immunocytochemistry. After immunocytochemistry, 4 random fields (157.5 × 210 mm rectangle) were captured per slide

Table 1 Information on primary and secondary antibodies for immunohisto- and cyto-chemistry

Primary antibody	Type	Dilution	Source; catalog
CD9	Rat monoclonal	1:100	SANTA CRUZ; sc-18869
CD81	Hamster monoclonal	1:100	Acris Antibodies GmbH; SM1526PS
SOX2	Goat monoclonal	1:100	Neuromics; GT15098
S100β	Rabbit monoclonal	1:100	Abcam; ab52642
CD81	Hamster monoclonal	1:100	Acris; SM1526PS
BrdU	Rabbit monoclonal	1:100	Rockland INC.; 600-401-C29S
GH	Rabbit polyclonal	1:10,000	*
PRL	Rabbit polyclonal	1:10,000	*
TSHβ	Rabbit polyclonal	1:10,000	*
LHβ	Rabbit polyclonal	1:10,000	*
ACTH	Rabbit polyclonal	1:10,000	*
Secondary antibody		**Dilution**	**Source; catalog**
Alexa Fluor 568-conjugated goat anti-rat IgG		1:200	Thermo Fisher Scientific; A-11077
Alexa Fluor 568-conjugated goat anti-mouse IgM		1:200	Thermo Fisher Scientific; A-21043
Alexa Fluor 568-conjugated donkey anti-mouse IgG		1:200	Thermo Fisher Scientific; A-10037
Alexa Fluor 568-conjugated goat anti-rabbit IgG		1:200	Thermo Fisher Scientific; A-11011
Alexa Fluor 488-conjugated donkey anti-goat IgG		1:200	Thermo Fisher Scientific; A-11055
Alexa Fluor 488-conjugated goat anti-rat IgG		1:200	Thermo Fisher Scientific; A-11006
Alexa Fluor 488-conjugated goat anti-rabbit IgG		1:200	Thermo Fisher Scientific; A-11008
Alexa Fluor 488-conjugated goat anti-hamster IgG		1:200	Thermo Fisher Scientific; A-21110

*Supplyer: Dr. A. F. Parlow, Scientific Director, National Hormone & Peptide Program (Rizzoti et al. 2013)

using a 40-fold objective lens. The number of CD9-positive cells and the total number of cells (DAPI) per area were counted by the cellSens Dimension system. Cell counts were performed three times for each experimental group.

Detection of AMCA-positive cells in primary culture of CD9-positive cells

We used the dipeptide-β-Ala-Lys-*Nε*-7-amino-4-methylcoumarin-3-acetic acid (AMCA, GenScript, Piscataway, NJ, USA) to detect S100β-positive cells. AMCA was added to the culture at a concentration of 40 µM, and cells were incubated for 2 h at 37 °C. To visualize the AMCA uptake together with CD9 expression, cells were further incubated with primary antibodies and processed as described above for immunocytochemistry.

qPCR

qPCR was performed as described previously (Horiguchi et al. 2018). Briefly, qPCR assays were conducted on a Thermal Cycler Dice Real Time System II (Takara Bio, Shiga, Japan) using gene-specific primers and SYBR Premix Ex Taq II (Takara) containing SYBR Green I. The sequences of the gene-specific primers are listed in Table 2. We also quantified β-actin (*Actb*) for normalisation. Relative gene expression was calculated by comparing cycle times for each target PCR. Cycle threshold values were converted to relative gene expression levels using the $2^{-(\Delta Ct\ sample - \Delta Ct\ control)}$ method.

Small interfering RNA (siRNA)

CD9-positive cells isolated from the anterior lobe of adult mice were plated at 1.0×10^5 cells/cm^2 on 8-well glass chamber slides with laminin-coated surfaces. Cells were then cultured for 24 h in 500 µL Medium 199 with 10% FBS (Merck Millipore, Darmstadt, Germany) at 37 °C in a humidified atmosphere of 5% CO_2 and 95% air. For siRNA transfection, the culture medium was replaced with 500 µL Medium 199 with 10% foetal bovine serum (FBS) supplemented with transfection reagent (INTERFERin at 1:100 v/v; PolyPlus Transfection, Illkirch, France) and siRNAs against *Cd9* and *Cd81* mRNA (0.2 µM Mm_*Cd9*_1 and Mm_*Cd81*_2; Qiagen, Venlo, Netherlands) in each well. A non-silencing siRNA without homology to any known mammalian gene was used as a negative control (SI03650325; Qiagen). After 48 h cultivation with siRNA reagents, cells were processed for proliferation assays and immunocytochemistry.

Proliferation assay

To quantify proliferative activity, the nucleotide analogue 5-bromo-2′-deoxyuridine (BrdU; Rockland Inc., Limerick, PA, USA) was added at a concentration of 3 µg/mL to the primary culture of 1.0×10^5 cells/cm^2 CD9-positive cells for 24 h after siRNA treatment. Cells were fixed in 4% paraformaldehyde in 0.025 M PB (pH 7.4) for 15 min at room temperature, and then treated with 4 N HCl in PBS for 10 min. Immunocytochemistry for BrdU was performed (Table 1), and ten images per well were randomly taken with a 40-fold objective lens. BrdU-positive cells and the total number of cells (DAPI) per area were counted with the cellSens Dimension system. Cell counts were performed three times for each experimental group.

Growth and differentiation of pituispheres

Isolated CD9-positive with or without *Cd9/Cd81* siRNA treatment, and -negative cells were plated on 35 mm untreated dishes (AGC TECHNO GLASS, Shizuoka, Japan) at a density of 40,000 cells/dish in DMEM/F-12 containing B27 supplement (1:50; Thermo Fisher Scientific, Waltham, MA, USA), N2 supplement (1:100; Wako, Osaka, Japan), bovine serum albumin (BSA, 0.5%; Sigma-Aldrich), basic fibroblast growth factor (bFGF, 20 ng/mL), and epidermal growth factor (EGF, 20 ng/mL). The cells were incubated

Table 2 Primers for qPCR

Mouse Genes	Forward sequence	Reverse sequence	Product size	Genbank accession no
Cd9	CCTGAAGCCATCAGTGAGGT	GCACAGGATCATGCTGAAGA	111	NM_007657
Cd81	GGCATATGTGGGATGTAGGG	CAAAGCCTCTGGGCAAGTAG	123	NM_133655
Sox2	CCATTTTCGTGGTCTTGTTT	TCAACCTGCATGGACATTTT	94	NM_001109181
S100β	ATGGGGAGTGTGACTTCCAG	CCCTCATGTCTGTTGCAGAA	145	NM_009115
Gh	TCCTGTGGACAGATCACTGC	GGGAAAAGCACTAGCCTCCT	110	NM_008117
Prl	TGGTTCTCTCAGGCCATCTT	ATTTTGGCAGAACAGCAGGT	130	X04418
Tshβ	GAGAGTGGGTCATCACAGCA	TTGAACAACCCCAGCTCTTC	129	NM_009432
Lhβ	GTCCCAGGACTCAACCAATG	GGGAGGGAGGGATGATTAGA	110	NM_008497
Pomc	GGGTCCCTCCAATCTTGTTT	GCACCAGCTCCACACATCTA	137	NM_001278581
Actb	TGGCACCACACCTTCTACAATGAGC	GGGTCATCTTTTCACGGTTGG	106	NM_007393

in humidified chambers with 5% CO_2 at 37 °C. Pituispheres were passaged by incubation in 0.05% trypsin with 5 mM EDTA in DMEM/F-12 containing 0.5% BSA for 20 min, and then mechanically dissociated into a single-cell suspension. This was followed by incubation on 35 mm untreated dishes, as described above, for another 5 days. Pituispheres were collected manually with pipettes under microscopic control. We counted the size and the number of each spheres after DAPI staining. Differentiation induction of pituispheres was performed by an overlay 3D culture method on Matrigel-coated 16-well chamber slides (0.4 cm^2/well) (Thermo Fisher Scientific). This was done with 20 ng/mL bFGF, EGF, and 20% KnockOut serum replacement (KSR, Thermo Fisher Scientific) for 4 days. This was then replaced with medium including BIO (GSK3β-inhibitor, 250 nM; Wako), and cultivation was continued for another 10 days.

Statistical analysis

Data are presented as the mean values ± SEM of at least three experiments for each group. The Student's *t* test (after the *F* test), and the Tukey–Kramer test were used for comparisons between two, and more than two groups, respectively. Differences were considered significant at $P < 0.05$.

Results

Identification of CD9/CD81-positive cells in the mouse anterior lobe

Frozen haematoxylin and eosin (H&E)-stained sections of adult mouse pituitary glands are shown in Fig. 1a. A stem/progenitor niche is defined as a microenvironment that maintains stem cells using growth factors, cell surface proteins, and extracellular matrix (ECM). In the adult anterior pituitary, SOX2-positive cells are identified in the primary (marginal cell layer (MCL) facing Rathke's cleft between the anterior and intermediate lobes) and secondary (parenchyma) stem/progenitor cell niches. The present study used immunohistochemistry to examine whether CD9 and CD81 are present in these niches. The results showed that CD9 and CD81 were co-localised in the MCL of the anterior and intermediate lobes and the parenchyma of the anterior lobe, but not in the posterior lobe (Fig. 1b). To determine the specificity of the anti-mouse CD9 antibody, we performed double staining using in situ hybridization for *Cd9* and immunohistochemistry for CD9. *Cd9*-expressing cells were immunopositive for CD9 (Supplementary Fig 1a), indicating that the CD9 antibody used in the present study is both specific and appropriate for immunohistochemistry to detect *Cd9*-expressing CD9-positive cells. Of note, the absence of anti-CD9 nonspecific immunoreaction was confirmed using a preabsorption control (the anti-CD9 antibody was preincubated with synthetic CD9, and the resultant supernatant was used as the preabsorbed antibody). While we observed *Cd9*-expressing cells in the MCL of the anterior and intermediate lobes and the parenchyma of the anterior lobe, no positive cells were seen when the preabsorbed antibody was used (Supplementary Fig 1b). Next, we focused on the anterior lobe and analysed the proportion of CD9-positive cells (among total 2,235 cells) in the MLC and parenchyma of the anterior lobe. The result was 4.9% (Fig. 1b, bottom table). H&E staining and immunofluorescence of the mouse pituitaries at embryonic day 10.5 (E10.5), 15.5, P0, and P5 are shown in Fig. 2. Although CD9- and CD81-positive cells were not detected during embryonic development (Fig. 2a), they were observed in the intermediate lobe and in some areas of the anterior lobe at P0 (Fig. 2b) and P5 (Fig. 2c).

Next, we performed double staining for CD9 and SOX2 (Fig. 3a) or S100β (Fig. 3b) in the anterior lobes of adult mice. The proportions of SOX2-positive cells among CD9-positive cells (1,635 cells) and CD9-positive cells among SOX2-positive cells (1434 cells) were 51.7% and 64.8%, respectively (Fig. 3a, bottom table), similar to the proportion of S100β-positive cells among SOX2-positive cells (approx. 60%, Andoniadou et al. 2013). The proportions of S100β-positive cells among CD9-positive cells (360 cells) and CD9-positive cells among S100β-positive cells (344 cells) were 87.2% and 91.5%, respectively (Fig. 3b, bottom table). Mouse S100β-positive cells (folliculo-stellate cells) can be identified as per the uptake of AMCA-labeled dipeptide (Krylyshkina et al. 2005). As shown in Supplementary Fig 2, almost all of AMCA-positive cells were CD9 positive.

Isolation of CD9-positive cells from the adult mouse anterior lobe

We next isolated CD9-positive cells from the adult mouse anterior lobes using an anti-mouse CD9 rat monoclonal antibody combined with a Universal pluriBead kit. Samples were then prepared for smear preparation. Smear preparations were processed for double-immunofluorescence for CD9 and CD81, SOX2, or S100β (Fig. 4a). The proportions of CD9-positive cells, CD9/CD81-positive cells, CD9/SOX2-positive cells, and CD9/S100β-positive cells in the CD9-positive cell fraction (1,295 cells) were 90.7%, 89.5%, 47.9%, and 89.2%, respectively (Fig. 4b). Conversely, the proportions of those in the CD9-negative cell fraction (5193 cells) were 0.2–0.7% (Fig. 4b). The proportions of CD9-negative/SOX2-positive and CD9-negative/S100β-positive cells in the CD9-negative cell fraction were also low (Fig. 4b). The proportions of hormone- (growth hormone [GH], prolactin [PRL], thyroid-stimulating hormone [TSH], luteinising hormone [LH], adrenocorticotropic hormone [ACTH]), VE-cadherin- (endothelial cells), and DESMIN-positive cells

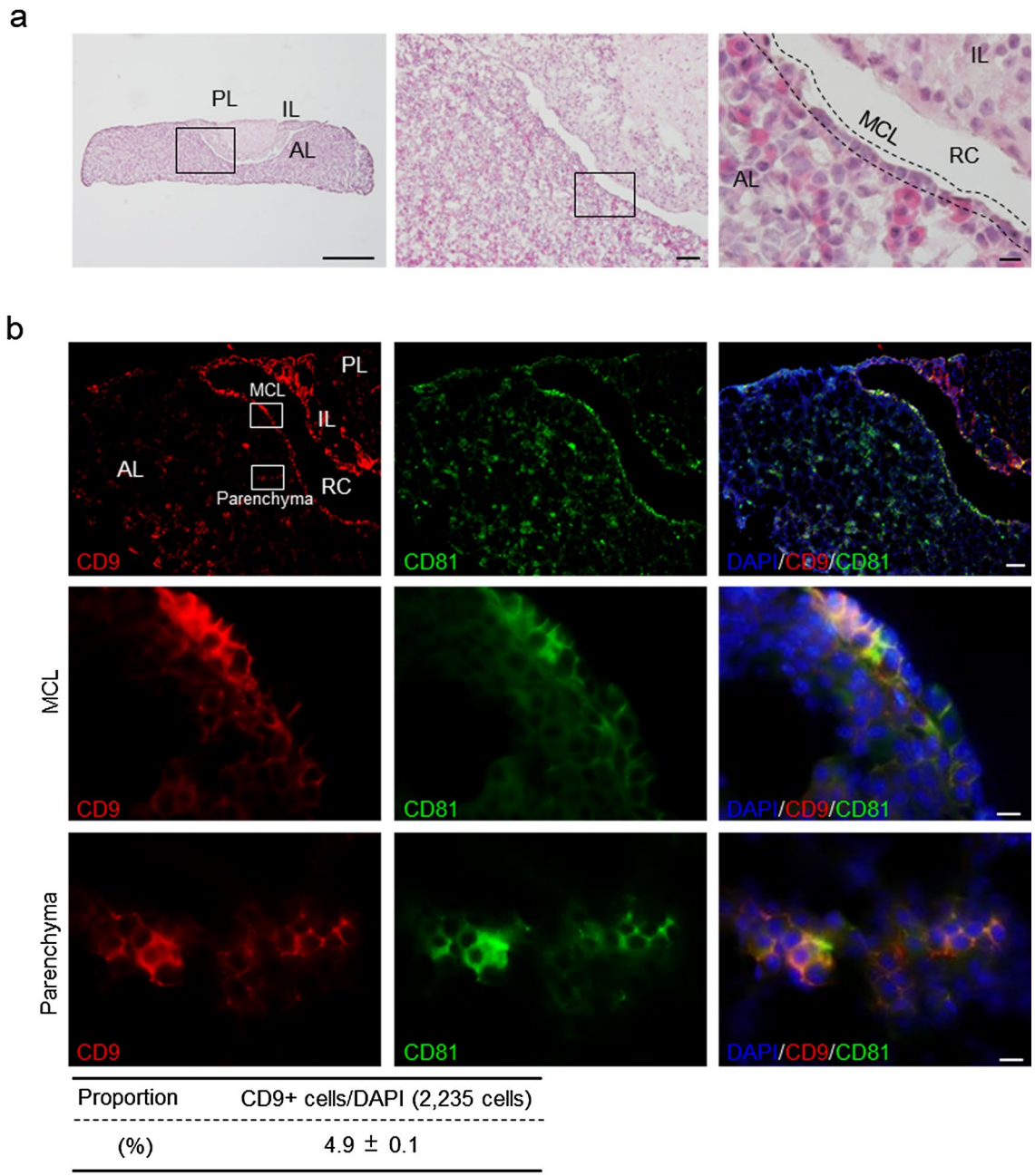

Fig. 1 Identification of CD9/CD81-positive cells in the anterior lobes of adult male mice. **a** Haematoxylin and eosin (H&E) staining of the pituitary gland. High magnification of boxed area in the left and middle panels is shown in the middle and right panels, respectively. **b** Double immunofluorescence for CD9 (red) and CD81 (green). High magnification of boxed area is shown in the second (marginal cell layer: MCL) and third rows (parenchyma). Right panels show merged images with DAPI (blue). Proportions of CD9-positive cells in the anterior lobe are shown in the bottom table (mean ± SEM, $n = 5$). *AL* anterior lobe, *IL* intermediate lobe, *PL* posterior lobe, *RC* Rathke's cleft. Scale bars 500 µm (**a** left panel), 200 µm (**b** upper panels), 100 µm (**a** middle panel), 20 µm (**a** right panel, **b** middle and bottom panels)

(pericytes) within CD9-positive cell fraction were lower than those in the CD9-negative cell fraction (Fig. 4b). qPCR analysis showed that the *Cd9* mRNA level was 4.5-fold higher in the CD9-positive cell fraction than in the CD9-negative cell fraction (Fig. 4c). In addition, the mRNA levels of *Cd81*, *Sox2*, and *S100β* were significantly higher, while the mRNA levels of all anterior pituitary hormones (*Gh*, *Prl*, *Tshβ*, *Lhβ*, and proopiomelanocortin [*Pomc*]) were significantly lower in the CD9-positive cell fraction than those in the CD9-negative cell fraction (Fig. 4c).

Effect of CD9 and CD81 siRNAs on proliferation

Our previous study using rats revealed that S100β-positive cells exhibited marked proliferation activity under the influence of laminin, an ECM component of the basement membrane, through ECM receptor integrins (Horiguchi et al. 2010). To examine the function of CD9 and CD81 in the mouse anterior lobe, we knocked down *Cd9* and/or *Cd81* gene expression using siRNAs in CD9-positive cells. These cells were primarily cultured on laminin-coated surfaces at 1.0×10^5 cells/cm^2. *Cd9* and/or *Cd81* expression levels were successfully downregulated by treatment with *Cd9* and/or *Cd81* siRNAs, respectively, whereas *Sox2* and *S100β* expression were unaffected (Fig. 5a). The number of BrdU-positive signals in cells treated with *Cd9* and *Cd81* siRNAs was clearly lower than that in control cells (Fig. 5b). In addition, the proportions of BrdU-positive cells in *Cd9* ($9.2 \pm 0.8\%$), *Cd81* ($8.0 \pm 0.6\%$), and *Cd9* and *Cd81* ($10.0 \pm 1.3\%$) siRNA-treated cells were significantly lower ($P < 0.01$) than that in control cells ($16.1 \pm 0.8\%$) (Fig. 5c).

Capacity for pituisphere formation and differentiation into hormone-producing cells in CD9-positive cells

To test the stem/progenitor cell potential of CD9-positive and -negative cells, non-adherent pituispheres were grown in culture (Fig. 6a). After a 5-day cultivation period, pituispheres were collected manually with pipettes under a microscope. We collected a total of 205 and 26 pituispheres from CD9-positive, and -negative cell fractions, respectively. The number of pituispheres in the CD9-positive cell fraction was higher than that in the CD9-negative cell fraction (Fig. 6b). However, the number of pituispheres, the size of pituispheres, and cell number in pituispheres of CD9-positive fraction was not significantly changed regardless of the presence or absence of *Cd9*/*Cd81* siRNA (Supplementary Fig 3). Pituispheres were able to be propagated after (enzymatic and mechanical) dissociation to form the second- and third-passage spheres (data not shown). After cultivation for 5 days, pituispheres from the CD9-positive cell fraction were immunopositive for CD9, S100β, and SOX2 (Fig. 6c). However, pituispheres from the CD9-negative cell fraction were immunonegative for CD9 and S100β, but positive for SOX2 (Fig. 6c). Of note, we observed using immunocytochemistry that no hormone-producing cells were contained within CD9-positive or CD9-negative pituispheres before induction (data not shown). In addition, we examined the differentiation capacity of the pituispheres using Matrigel-coated glass slides and serum-free medium with bFGF, EGF, KSR, and GSK3β inhibitors (Yoshida et al. 2016). Pituisphere differentiation was induced by the overlay 3D culture method on Matrigel-coated 16-well chamber slides for 14 days (with medium changes at days 2, 4, 7, 11, and 14). After induction, the pituispheres from the CD9-positive and CD9-negative cell fractions were reactive to a cocktail of antibodies to various hormones (GH/PRL/TSHβ/LHβ/ACTH) (Fig. 7a). The proportion of GH/PRL/TSHβ/LHβ/ACTH-positive cells in the pituisphere was higher in the CD9-positive cell fraction ($18.0 \pm 1.5\%$) than that in the CD9-negative cell fraction ($6.6 \pm 1.1\%$, Fig. 7b). Of note, we confirmed to stain induced-pituispheres from CD9-positive fraction (Fig. 7c) and CD9-negative fraction (Supplementary Fig 4) with each anti-anterior pituitary hormone antibody (GH, PRL, TSHβ, LHβ, and ACTH). The result showed that the pituispheres had differentiation capacity to all types of hormone-producing cells. CD9/GH-positive or CD9/PRL-positive cells also appeared in the pituispheres from the CD9-positive cell fraction (Fig. 7c, white arrowheads). Additionally, CD9/S100β-positive cells were observed in the pituispheres of the CD9-positive cell fraction (Fig. 7c, white arrowheads). Of note, S100β-positive cells were observed after CD9-negative pituisphere induction (Supplementary Fig 4). However, it is unclear whether CD9-negative cells differentiate into S100β-positive cells.

Discussion

In the present study, we demonstrated that *Cd9* and *Cd81* were expressed in SOX2/S100β-positive cells of the mouse anterior lobe after birth. We succeeded in isolating CD9-positive cells with more than 90% purity from the anterior lobes of adult mice. These had the capacity to form pituispheres and differentiate into all types of hormone-producing cells.

The anterior lobe contains five types (GH, PRL, TSH, LH/FSH, and ACTH) of hormone-producing cells, together with non-hormonal cells such as S100β-positive cells, endothelial cells, and pericytes. S100β-positive cells are localised in the MCL, which faces the residual lumen of Rathke's cleft, and also form cell clusters in the parenchyma of the anterior lobe (Inoue et al. 1999). It is reported that the proportion of S100β-positive cells in the anterior lobe is approximately 5% (Sato and Inoue 2000). The present study showed that approximately 90% of S100β-positive cells were immunopositive for CD9 and CD81, and that the proportion of CD9/CD81-positive cells in the adult anterior lobe of mice was 4.9%. This indicates that most S100β-positive cells expressed *Cd9* and *Cd81*. Immunohistochemistry and immunocytochemistry revealed that CD9/SOX2-positive cells were 51.7% of the total SOX2-positive cells in the anterior lobe and 47.9% of the isolated CD9-positive cell

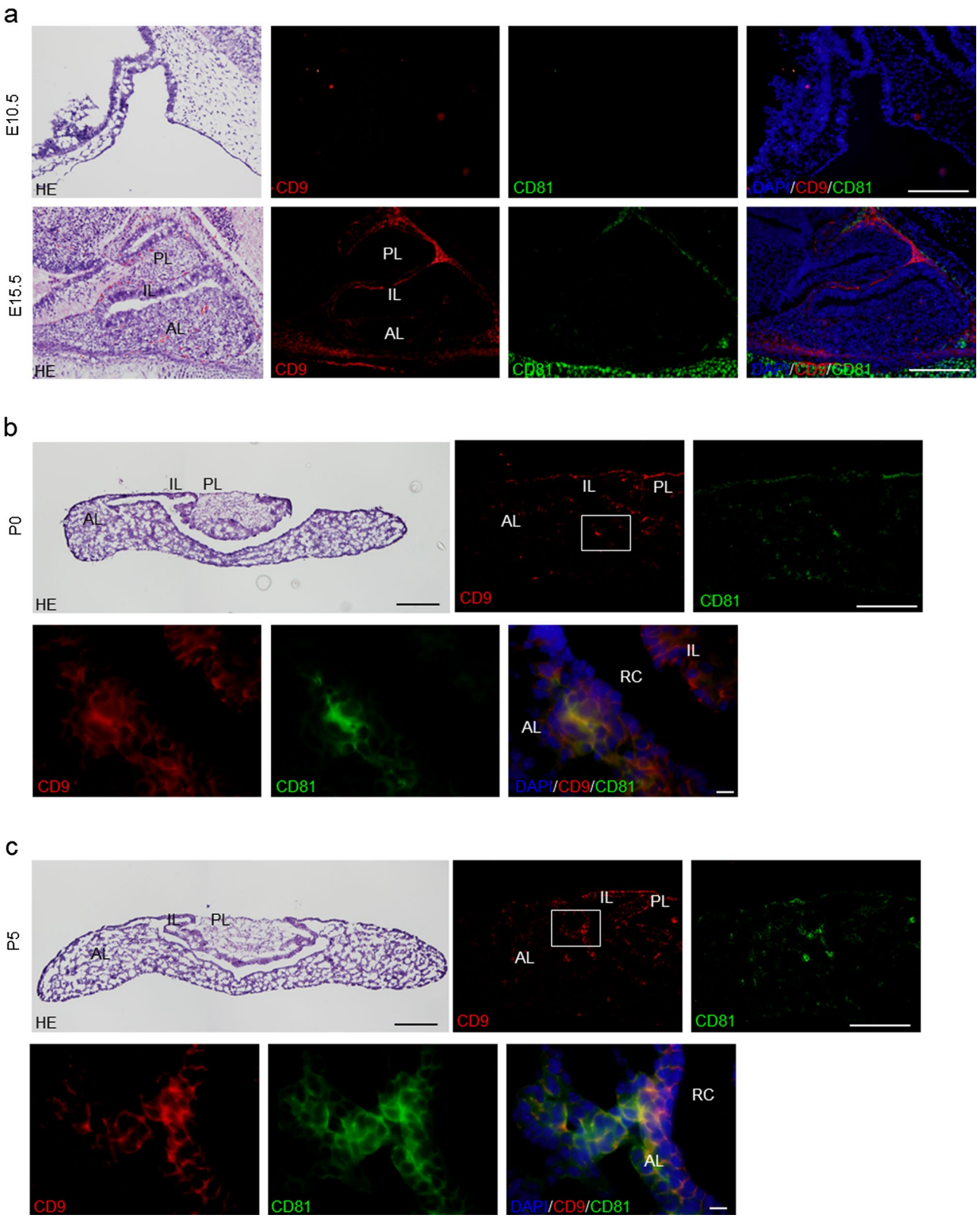
a
E10.5
HE
CD9
CD81
DAPI/CD9/CD81
E15.5
PL
IL
AL
HE
CD9
CD81
DAPI/CD9/CD81
b
P0
IL
PL
AL
HE
CD9
CD81
RC
DAPI/CD9/CD81
c
P5
IL
PL
AL
HE
CD9
CD81
RC
DAPI/CD9/CD81

◂**Fig. 2** Identification of CD9/CD81-positive cells in the developing mouse anterior lobe. **a** Sagittal view of embryonic pituitaries at embryonic day 10.5 (E10.5) (top) and E15.5 (bottom). Haematoxylin and eosin (H&E) staining (left panels) and immunofluorescence for CD9 (red) and CD81 (green) are shown. Right panels are merged images with DAPI (blue). **b**, **c** Frontal view of postnatal pituitaries at postnatal day 0 (P0) and P5. H&E staining (left in the first row) and immunofluorescence for CD9 (red) and CD81 (green) are shown. High magnification of boxed area is shown in each second row (right: merged images with DAPI, blue). *AL* anterior lobe, *IL* intermediate lobe, *PL* posterior lobe, *RC* Rathke's cleft. Scale bars 200 µm (**a**, and upper panels of **b** and **c**), 10 µm (bottom panels of **b** and **c**)

fraction. We therefore identified CD9 as a novel marker for S100β-positive cells in the anterior lobes of adult mice. By using an anti-CD9 antibody, we also successfully established an isolation method without expensive cell sorting devices or transgenic animals. In the future, this method could be a useful and convenient tool for investigating the functions of S100β-positive cells in mice.

CD9 and CD81 have been implicated in sperm-egg fusion, cell migration, tumour cells, metastasis, nervous system development, and cell proliferation (Boucheix and Rubinstein 2001). The present study showed that S100β/SOX2-positive cell proliferation was inhibited via the treatment with siRNAs targeting *Cd9* and/or *Cd81*. Our previous study using rats showed that in S100β/SOX2-positive cells, CD9 and CD81 sustain proliferation activity through integrin signalling, and that *Cd9* downregulation triggers CD9-positive cell migration or differentiation (Horiguchi et al. 2018). Similar mechanisms may exist in mouse CD9/CD81/SOX2/S100β-positive cells.

The development of hormone-producing cells in the anterior lobe is currently poorly understood. Gleiberman et al. (2008) have hypothesised that the adult anterior lobe is composed of two different terminally differentiated endocrine cell types originating from embryonic and adult stem cells (Gleiberman et al. 2008). This suggests that both cells are present in the adult anterior lobe as sources of hormone-producing cells. However, no molecular markers that can distinguish embryonic precursors from adult stem cells have been found. Accumulating evidence indicates that S100β-positive cells act as stem/progenitor cells in the anterior lobe (Allaerts and Vankelecom 2005). Approximately 60% of S100β-positive cells are immunopositive for the stem/progenitor marker SOX2. These data strongly suggest that SOX2-positive cells can be categorised into subpopulations in the presence or absence of S100β. The present study showed that CD9 is a novel marker for S100β-positive cells, and that CD9/CD81-positive cells began appearing in the anterior lobe after birth. Furthermore, isolated CD9-positive cells showed their capacity to form pituispheres and to differentiate into endocrine cells in a similar three-dimensional cultivation system. The present results can explain the phenotypes of atrophy in the anterior lobe and small numbers of acidophilic cells in CD9/CD81 DKO mice without significant growth abnormality until 3 weeks of age (Jin et al. 2018). These findings suggest that CD9/CD81/SOX2/S100β-positive cells can act as adult stem cells in the anterior lobe of the pituitary. Further study using CD9/CD81 DKO mice may contribute to a deeper understanding of the adult stem cells and their functions in the anterior lobe.

On the other hand, CD9-negative, SOX2-positive, and S100β-negative cells (CD9-/SOX2+/100β-cells) in the CD9-negative cell fraction also had the capacity to form pituispheres and to differentiate into hormone-producing and S100β-positive cells. Although further study is required, CD9/CD81/SOX2/S100β-positive cells could either originate from CD9-/SOX2+/100β- cells or be another subpopulation of SOX2-positive cells.

In conclusion, we found that approximately half of CD9/CD81-positive cells expressed S100β and SOX2 in the mouse pituitary gland. Further, CD9 and CD81 contributed to sustaining the proliferation ability of CD9/CD81/S100β/SOX2-positive cells. Isolated CD9-positive cells had pituisphere formation capacity and were able to differentiate into hormone-producing cells. These findings can provide a better understanding of adult tissue stem cells and the development of hormone-producing cells in the anterior lobe.

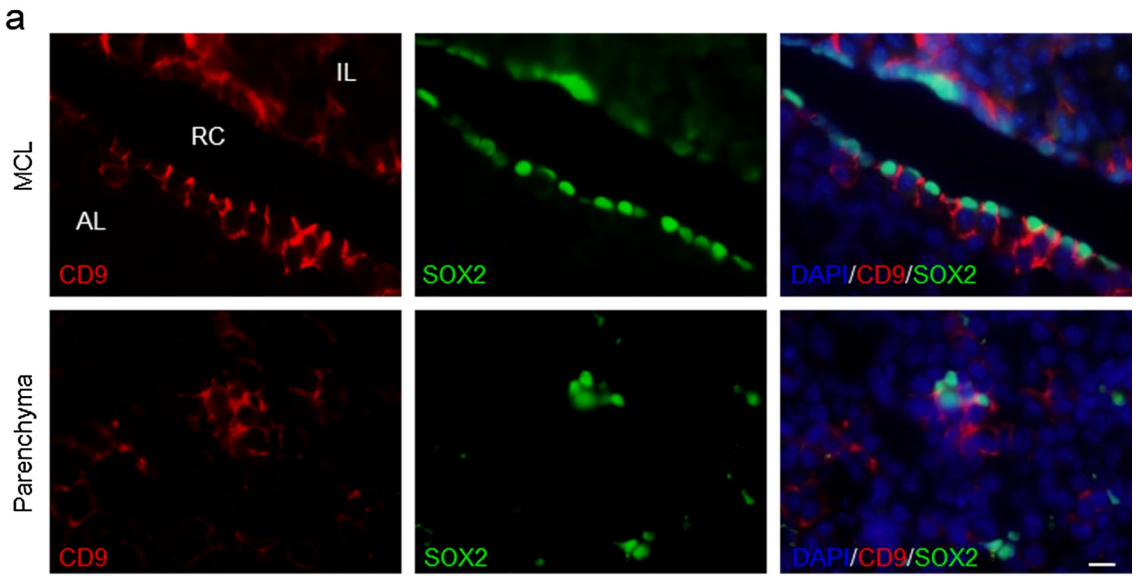

Proportion	SOX2+ cells/CD9+ cells (1,635 cells)	CD9+ cells/SOX2+ cells (1,434 cells)
(%)	51.7 ± 0.8	64.8 ± 1.0

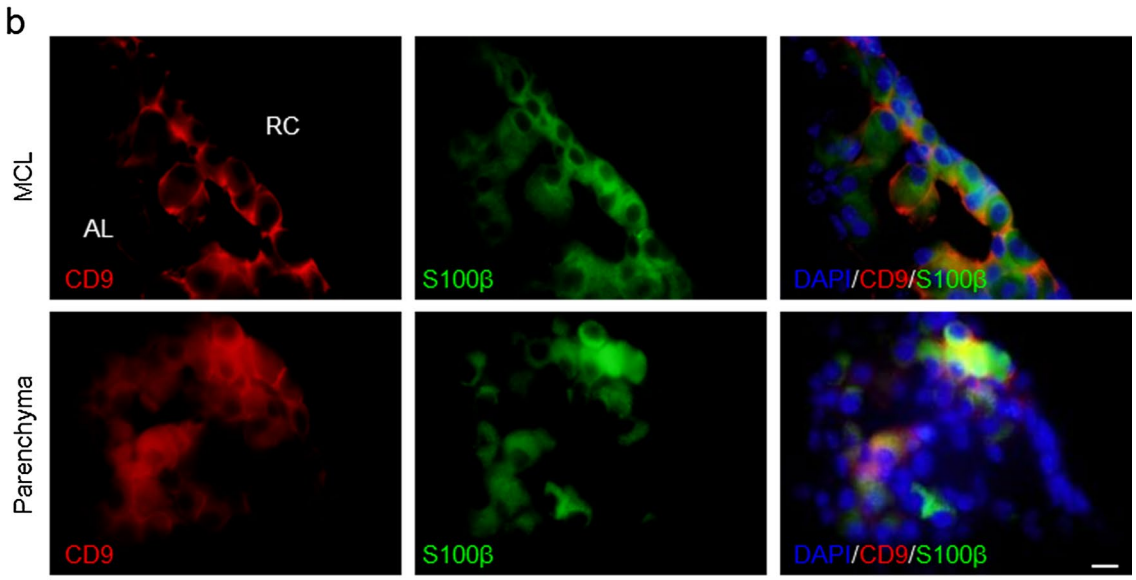

Proportion	S100β+ cells/CD9+ cells (360 cells)	CD9+ cells/S100β+ cells (344 cells)
(%)	87.2 ± 0.9	91.5 ± 2.2

Fig. 3 Proportion of SOX2 and S100β-positive cells amongst CD9-positive cells in the marginal cell layer (MCL) and parenchyma of the anterior lobe (**a** and **b**). Double immunofluorescence for CD9 (red) and SOX2 (**a**, green) or S100β (**b**, green). Right panels are merged images with DAPI (blue). Proportions of SOX2 or S100β-positive cells among CD9-positive cells or CD9-positive cells among SOX2- or S100β- positive cells are shown in each bottom table (mean ± SEM, $n = 5$). *AL* anterior lobe, *IL* intermediate lobe, *RC* Rathke's cleft. Scale bars 20 µm

a

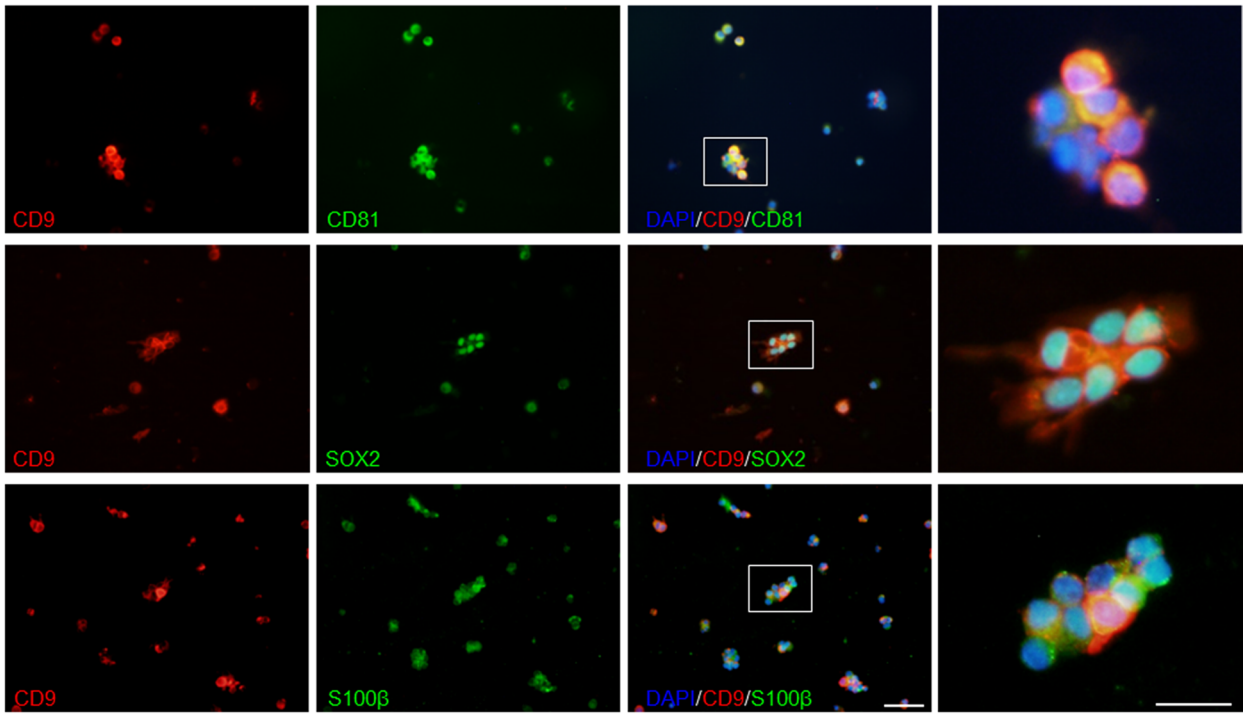

b

	CD9+ cell fraction (%, per 1,295 cells)	CD9- cell fraction (%, per 5,193 cells)
CD9+	90.7 ± 1.3	0.7 ± 0.0
CD9+/CD81+	89.5 ± 0.3	0.7 ± 0.0
CD9+/SOX2+	47.9 ± 3.1	0.2 ± 0.3
CD9-/SOX2+	1.1 ± 0.8	5.2 ± 0.7
CD9+/S100β+	89.2 ± 0.3	0.5 ± 0.3
CD9-/S100β+	0.9 ± 0.3	0.5 ± 0.3
GH+	4.0 ± 1.0	38.0 ± 3.4
PRL+	2.1 ± 1.2	22.3 ± 1.0
TSH+	2.0 ± 0.1	9.9 ± 1.2
LH+	1.1 ± 1.2	5.4 ± 1.1
ACTH+	2.1 ± 1.1	10.7 ± 1.4
VE-Cadherin+	2.1 ± 1.3	7.0 ± 0.7
Desmin+	1.6 ± 0.8	4.5 ± 0.7

c

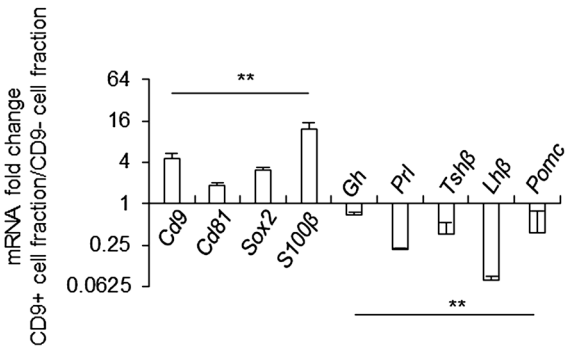

Fig. 4 Isolation of CD9-positive cells from the mouse anterior lobe. **a** Immunofluorescence for CD9 (*red*), CD81 (first row, green), SOX2 (second row, green) and S100β (third row, green) using smear preparation of the CD9-positive fraction. The third panels from the left are merged images with DAPI (blue). The right panels are the high magnifications of the boxed areas in merged images. Scale bars, 50 µm and 100 µm (right panel). **b** Proportions of immunoreactive cells (CD9+, CD9−, CD81+, SOX2+, S100β+, GH+, PRL+, TSH+, LH+, ACTH+, VE-cadherin+, and Desmin+) in the CD9-positive or CD9-negative cell fraction (mean ± SEM, $n = 5$). **c** Relative mRNA levels in CD9-positive cells against those of CD9-negative cells (mean ± SEM, $n = 3$). Data were normalised with an internal control (*Actb*). Graphs represent *Cd9*, *Cd81*, *Sox2*, and *S100β,* and *Gh*, *Prl, Tshβ, Lhβ*, and *Pomc*. $^{**}P < 0.01$

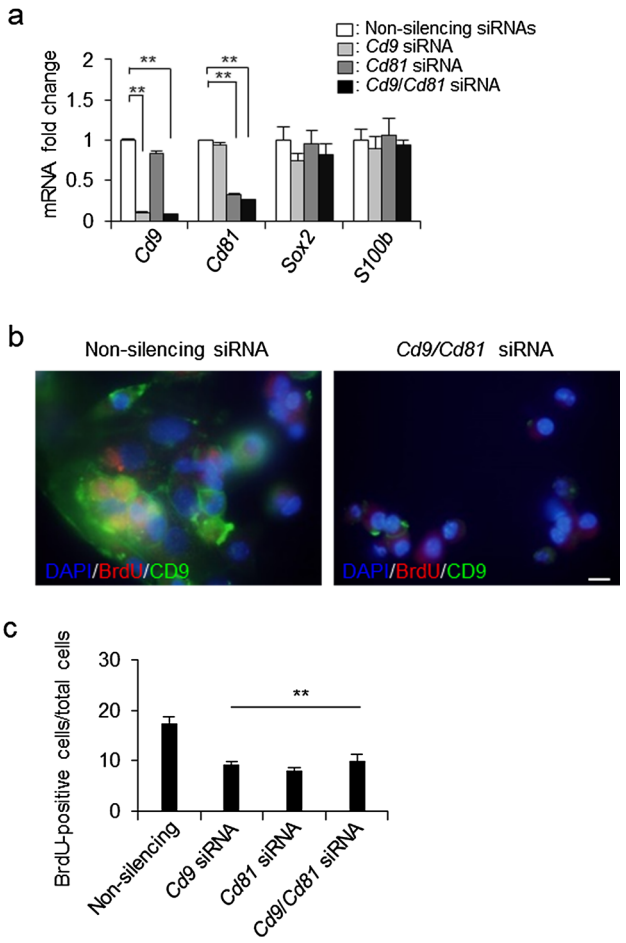

Fig. 5 Downregulation of *Cd9* and *Cd81* mRNA levels by siRNA transfection in CD9-positive cells **a** *Cd9*, *Cd81*, *Sox2*, and *S100β* mRNA levels in CD9-positive cells after 48 h treatment with non-silencing siRNAs (white), *Cd9* (*Cd9* siRNA, gray), *Cd81* (*Cd81* siRNA, dark gray), or *Cd9* and *Cd81*-siRNAs (*Cd9*/*Cd81* siRNA, black) (mean ± SEM, $n = 3$). Data were normalised with an internal control (*Actb*). $^{**}P < 0.01$. **b** Immunocytochemistry for BrdU (red) and CD9 (green) after treatment of CD9-positive cells with siRNAs (left: non-silencing siRNA, right: *Cd9/Cd81 siRNA*). Scale bar 20 µm. **c** The ratio of BrdU-positive cells amongst CD9-positive cells in each siRNA treatment. $^{**}P < 0.01$

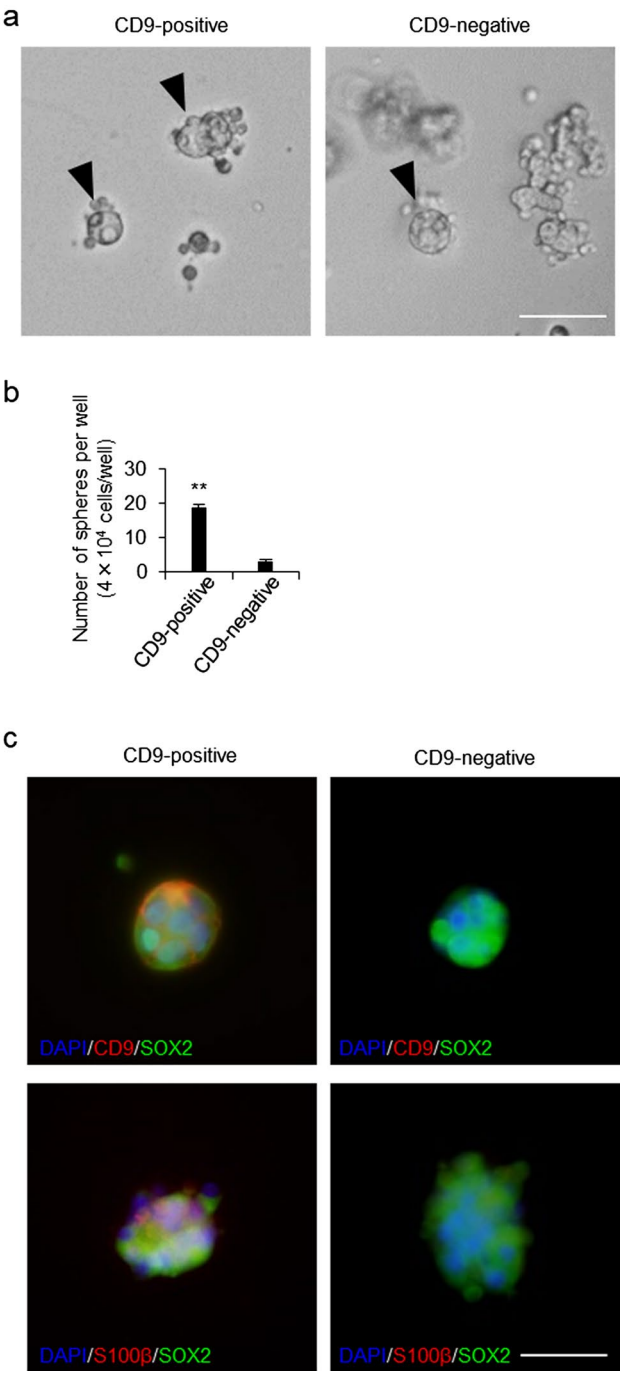

Fig. 6 Capacity for pituisphere formation in CD9-positive and CD9-negative cells. **a** Bright image of pituispheres (arrowheads). **b** The number of pituispheres formed in CD9-positive and -negative cell culture. **c** Double immunofluorescence for CD9 (red) and SOX2 (green) or S100β (red) and SOX2 (green) using CD9-positive and CD9-negative pituispheres. Scale bars 100 µm (**a**), 50 µm (**c**). $^{**}P < 0.01$

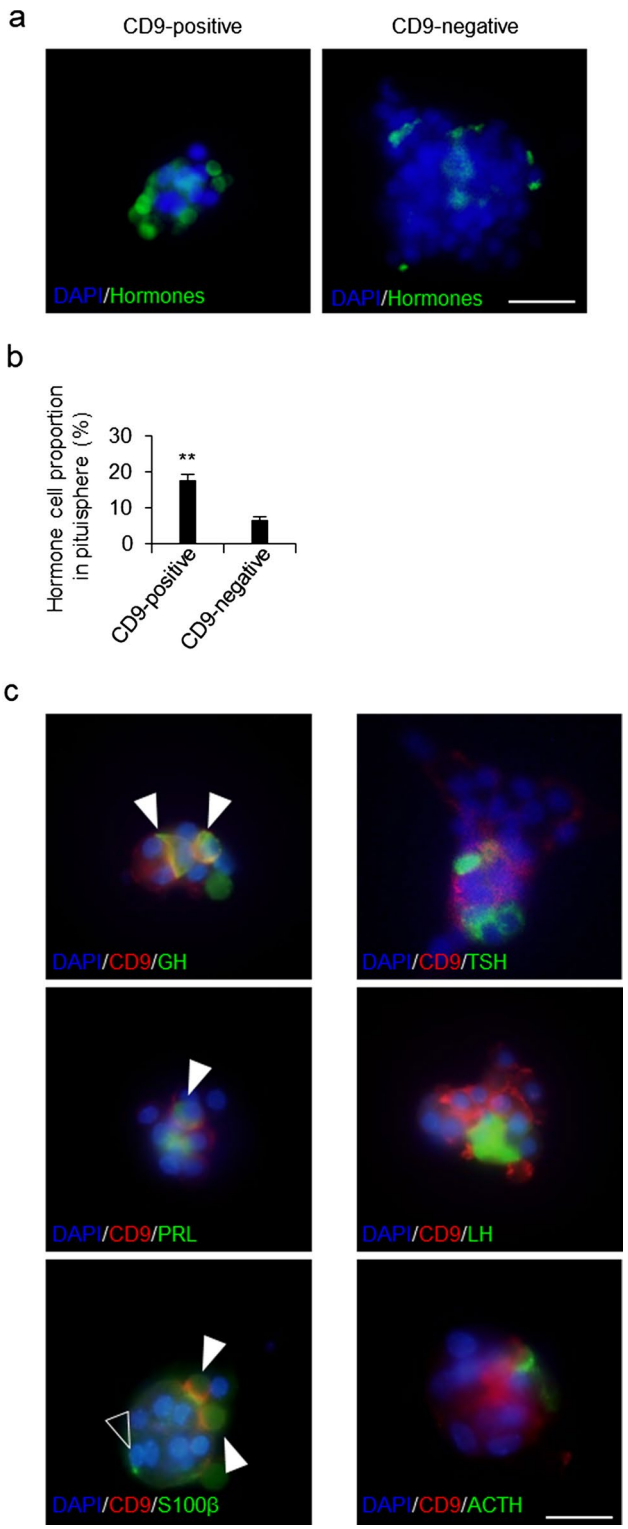

Fig. 7 Induction of differentiation into hormone-producing cells using CD9-positive and CD9-negative pituispheres **a** immunofluorescence for hormone cocktail antibodies (green) and DAPI (blue). **b** Proportion of hormone-producing cells in CD9-positive and CD9-negative pituispheres after induction. **c** Merged image of DAPI (blue), double-immunofluorescence against CD9 (red), and GH (green), PRL (green), S100β (green), TSH (green), LH (green), or ACTH (green) after induction are shown. White and black arrowheads indicate double-positive cells and single-positive cells, respectively. Scale bars, 50 µm (**a**, **c**). $^{**}P < 0.01$

Acknowledgements We would like to thank Dr. A. F. Parlow, Scientific Director, National Hormone & Peptide Program for kindly supplying the mouse GH, PRL, TSHβ, LHβ, and ACTH antibodies. We are grateful to Dr. T. Kato and Y. Kato (Institute for Reproduction and Endocrinology, Meiji University) for helpful discussions. We would like to thank Editage (www.editage.jp) for English language editing.

Funding This work was supported by JSPS KAKENHI Grants (no. 16K08475 and 19K 07255 to K.H., no. 17K08517 to K.F.).

Compliance with ethical standards

Conflict of interest The authors have no conflict of interest that might affect the impartiality of this research.

Ethics approval The current study was approved by the Committee on Animal Experiments of Kyorin University based on the NIH Guidelines for the Care and Use of Laboratory Animals. This article does not contain any studies with human participants. This article does not contain any studies with human participants or animals performed by any of the authors.

References

Allaerts W, Vankelecom H (2005) History and perspectives of pituitary folliculo-stellate cell research. Eur J Endocrinol 153:1–12

Andoniadou CL, Matsushima D, Mousavy Gharavy SN, Signore M, Mackintosh AI, Schaeffer M, Gaston-Massuet C, Mollard P, Jacques TS, Le Tissier P, Dattani MT, Pevny LH, Martinez-Barbera JP (2013) Sox2(+) stem/progenitor cells in the adult mouse pituitary support organ homeostasis and have tumor-inducing potential. Cell Stem Cell 13:433–445

Boucheix C, Rubinstein E (2001) Tetraspanins. Cell Mol Life Sci 58:1189–1205

Fauquier T, Rizzoti K, Dattani M, Lovell-Badge R, Robinson IC (2008) SOX2-expressing progenitor cells generate all of the major cell types in the adult mouse pituitary gland. Proc Natl Acad Sci USA 105:2907–2912

Gleiberman AS, Michurina T, Encinas JM, Roig JL, Krasnov P, Balordi F, Fishell G, Rosenfeld MG, Enikolopov G (2008) Genetic approaches identify adult pituitary stem cells. Proc Natl Acad Sci USA 105:6332–6337

Krylyshkina O, Chen J, Mebis L, Denef C, Vankelecom H (2005) Nestin-immunoreactive cells in rat pituitary are neither hormonal nor typical folliculo-stellate cells. Endocrinology 146:2376–2387

Higuchi M, Kanno N, Yoshida S, Ueharu H, Chen M, Yako H, Shibuya S, Sekita M, Tsuda M, Mitsuishi H, Nishimura N, Kato T, Kato Y (2014) GFP-expressing S100beta-positive cells of the rat anterior pituitary differentiate into hormone-producing cells. Cell Tissue Res 357:767–779

Horiguchi K, Fujiwara K, Yoshida S, Nakakura T, Arae K, Tsukada T, Hasegawa R, Takigami S, Ohsako S, Yashiro T, Kato T, Kato Y (2018) Isolation and characterisation of CD9-positive pituitary adult stem/progenitor cells in rats. Sci Rep 8:5533

Horiguchi K, Fujiwara K, Yoshida S, Tsukada T, Hasegawa R, Takigami S, Ohsako S, Yashiro T, Kato T, Kato Y (2020) CX3CL1/CX3CR1-signalling in the CD9/S100β/SOX2-positive adult pituitary stem/progenitor cells modulates differentiation into endothelial cells. Histochem Cell Biol 153:385–396

Horiguchi K, Yoshida S, Tsukada T, Nakakura T, Fujiwara K, Hasegawa R, Takigami S, Ohsako S (2020) Expression and functions of cluster of differentiation 9 and 81 in rat mammary epithelial cells. J Reprod Dev. https://doi.org/10.1262/jrd.2020-082 ((**Online ahead of print**))

Horiguchi K, Kikuchi M, Kusumoto K, Fujiwara K, Kouki T, Kawanishi K, Yashiro T (2010) Living-cell imaging of transgenic rat anterior pituitary cells in primary culture reveals novel characteristics of folliculo-stellate cells. J Endocrinol 204:115–123

Inoue K, Couch EF, Takano K, Ogawa S (1999) The structure and function of folliculo-stellate cells in the anterior pituitary gland. Arch Histol Cytol 62:205–218

Jin Y, Takeda Y, Kondo Y, Tripathi LP, Kang S, Takeshita H, Kuhara H, Maeda Y, Higashiguchi M, Miyake K, Morimura O, Koba T, Hayama Y, Koyama S, Nakanishi K, Iwasaki T, Tetsumoto S, Tsujino K, Kuroyama M, Iwahori K, Hirata H, Takimoto T, Suzuki M, Nagatomo I, Sugimoto K, Fujii Y, Kida H, Mizuguchi K, Ito M, Kijima T, Rakugi H, Mekada E, Tachibana I, Kumanogoh A (2018) Double deletion of tetraspanins CD9 and CD81 in mice leads to a syndrome resembling accelerated aging. Sci Rep 8:5145

Rizzoti K, Akiyama H, Lovell-Badge R (2013) Mobilized adult pituitary stem cells contribute to endocrine regeneration in response to physiological demand. Cell Stem Cell 13:419–432

Sato T, Inoue K (2000) Dendritic cells in the rat pituitary gland evaluated by the use of monoclonal antibodies and electron microscopy. Arch Histol Cytol 63:291–303

Susa T, Kato T, Yoshida S, Yako H, Higuchi M, Kato Y (2012) Paired-related homeodomain proteins Prx1 and Prx2 are expressed in embryonic pituitary stem/progenitor cells and may be involved in the early stage of pituitary differentiation. J Neuroendocrinol 24:1201–1212

Vila-Porcile E (1972) The network of the folliculo-stellate cells and the follicles of the adenohypophysis in the rat (pars distalis). Z Zellforch Microsk Anat Histochem 129:328–369

Yoshida S, Kato T, Yako H, Susa T, Cai LY, Osuna M, Inoue K, Kato Y (2011) Significant quantitative and qualitative transition in pituitary stem/progenitor cells occurs during the postnatal development of the rat anterior pituitary. J Neuroendocrinol 23:933–943

Yoshida S, Nishimura N, Ueharu H, Kanno N, Higuchi M, Horiguchi K, Kato T, Kato Y (2016) Isolation of adult pituitary stem/progenitor cell clusters located in the parenchyma of the rat anterior lobe. Stem Cell Res 17:318–329